Phase lapses in open quantum systems and the non-Hermitian Hamilton operator

Markus Müller[1,2] and Ingrid Rotter[2]
[1]*Facultad de Ciencias, Universidad Autónoma del Estado de Morelos, 62210 Cuernavaca, Morelos, Mexico*
[2]*Max-Planck-Institut für Physik komplexer Systeme, D-01187 Dresden, Germany*
(Received 8 December 2008; published 14 October 2009)

We study transmission through a system with $N=10$ states coupled to $K=2$ continua of scattering wave functions in the framework of the S matrix theory by using the Feshbach projection operator formalism for open quantum systems. Due to the coupling of the system (being localized in space) to the (extended) continuum of scattering wave functions, the Hamilton operator $H_{\rm eff}$ of the system is non-Hermitian. The numerical calculations are performed for different distributions of both the positions E_i^0 $(i=1,\ldots,N)$ of the states of the isolated (closed) system and the elements of the coupling vectors V^c between system and continua $(c=1,\ldots,K)$. The overall coupling strength α simulating the degree of resonance overlapping, is used as a parameter. In all cases, the complex eigenvalues and eigenfunctions of $H_{\rm eff}$ are controlled by α. In the regime of overlapping resonances, the well-known spectroscopic reordering processes (resonance trapping) take place because the phases of the eigenfunctions of $H_{\rm eff}$ are not rigid in the neighborhood of singular points (being crossing points of eigenvalue trajectories). Finally, width bifurcation generates $K=2$ short-lived and $N-K$ trapped long-lived states. Thus, narrow (Fano-like) resonances may appear in the transmission at high level density. They are similar to, but different from the Fano resonances in the scattering theory with $K=1$. Phase lapses are related to zeros in the transmission probability. Their number and position (in energy) are determined by the V^c and E_i^0, but not by α. However, number and position of the resonance states depend on α due to resonance trapping occurring in the regime of overlapping resonances. As a consequence, universal phase lapses between every two resonances may appear at high level density while the system will show mesoscopic features at low level density. The phase lapses are not a single phenomenon. Due to their link to singularities in the continuum, they are related also to other "puzzling" experimental results such as dephasing at low temperature.

DOI: 10.1103/PhysRevA.80.042705 PACS number(s): 03.65.Nk, 03.65.Vf, 03.65.Xp, 05.60.Gg

I. INTRODUCTION

In experiments [1–3] on Aharonov-Bohm rings containing a quantum dot in one arm, both the phase and magnitude of the transmission amplitude $T=|T|e^{i\beta}$ of the dot can be extracted. The results obtained caused much discussion since they did not fit into the general understanding of the transmission process. As a function of the plunger gate voltage V_g, a series of well-separated transmission peaks of rather similar width and height has been observed and, according to expectations, the transmission phases $\beta(V_g)$ increase continuously by π across every resonance. In contrast to expectations, however, β always jumps sharply downwards by π in each valley between any two successive peaks. These jumps called phase lapses, were observed in a large succession of valleys for every many-electron dot studied. The problem is considered theoretically in many papers [4–15].

In the most recent experiment [3], the transmission is studied not only through many-electron dots but also through few-electron ones. In the last case, the expected so-called mesoscopic behavior is observed: the phases are sensitive to details of the dot's configuration such as, e.g., the potential. In this regime, universal phase lapses between every two resonances are not observed. The main difference between few-electron and many-electron dots is that the level spacings are smaller in the latter case than in the first one such that the degree of resonance overlapping (ratio of average level spacing δ to average level width Γ) is different in the two cases [13,14]. Using the numerical and functional renormalization group approaches, systems with up to four levels are studied for different values δ/Γ. If $\delta \leq \Gamma$, one of the renormalized effective single-particle levels is typically a factor of 2 or 3 wider than the second widest, while the remaining 1 or 2 levels are very narrow [13]. For $\delta \geq \Gamma$, the phase $\beta(V_g)$ behaves mesoscopically. Universal phase lapses appear, in these calculations, only in the regime of overlapping resonances. This result is in qualitative agreement with the experimental ones.

The formation of broad (short-lived) states together with narrow (long-lived trapped) ones in the overlapping regime is well known for a long time, see e.g., the recent review [16]. This so-called trapping effect is generic. It appears in the regime of overlapping resonances under the influence of the environment. It is studied analytically as well as numerically in different small open quantum systems such as nuclei, atoms, quantum dots. It is found experimentally on a microwave cavity [17]. Mathematically, it can be linked to singularities in the continuum at which two (or more) eigenvalues of the non-Hermitian Hamilton operator coalesce.

It is the aim of the present paper to show that the phase lapses are related to the phenomenon of resonance trapping. Our study is based on the S matrix together with the concept of the Feshbach projection operator (FPO) formalism. In this formalism, the Hamiltonian of the system is non-Hermitian. We show that the phase lapses are a generic phenomenon appearing at high level density and that they are related to other "puzzling" phenomena observed experimentally on small quantum systems. Furthermore, we show that Fano-like resonances may appear also in the transmission. They

are however different from the Fano resonances in the one-continuum case of the scattering theory.

The FPO formalism is formulated about 50 years ago in nuclear physics for the description of nucleon-induced reactions on heavy nuclei with formation of compound nucleus states. Due to their high level density (about 10^6 states in an energy interval characteristic of single-particle resonances), the compound nucleus states as well as their coupling coefficients to the continuum are described usually by using statistical approaches [18]. In reactions on light nuclei however and in other studies on small systems, the basic equations of the FPO formalism can be solved directly without any statistical assumptions [16]. The crossover from low to high level density can therefore be controlled. Most important process in the crossover region is the *alignment* of a few resonance states to the states of the environment (continua of scattering wave functions) [19] and the decoupling (to some extent) of the other resonance states from the environment (*resonance trapping*). This phenomenon is described by the non-Hermitian Hamilton operator of the open system. It leads to changes in observable values, e.g., to an enhancement and acceleration of the transmission in the regime of overlapping resonances [16,20,21].

The interaction between the particles of the system is taken into account in these calculations in the same manner as in standard (conventional) calculations for the corresponding closed quantum system, see [16]. It influences the details of the calculation, but not the generic features. The widths of distant resonance states show usually the so-called mesoscopic behavior, i.e., the widths of *all* individual resonance states differ, although being of the same order of magnitude, relatively strongly from one another. The situation is another one in the regime of overlapping resonances. Here, a few broad short-lived modes are formed while the remaining states in this energy region become long-lived (trapped) and are characterized by small decay widths which are similar to one another. The phenomenon of resonance trapping causes a dynamical phase transition in the system [16]. An environmentally induced dynamical quantum phase transition is observed recently also in experimental and theoretical quantum chemistry studies [22].

In Sec. II, we sketch the FPO formalism and the S matrix derived within this framework. A central role in the formalism plays the non-Hermitian effective Hamilton operator $\widetilde{H}_{\rm eff}$. This operator describes the open quantum system, i.e., it takes into account the coupling of the states via the common continuum of scattering wave functions. In order to study *generic* features of open quantum systems, we approximate $\widetilde{H}_{\rm eff}$ by a simple expression for a toy model in which the overall coupling strength between system and environment can be controlled by means of the parameter α. In the framework of this model, the cross section including its phase can easily be calculated.

In Sec. III, we show numerical results obtained in the two-continua case ($K=2$) with $N=10$ resonance states and regular as well as random coupling coefficients V_i^c of the discrete states to the continuum. We are interested above all in the transmission through the system when the two attached leads are identical. We consider the phase of the transmission as a function of either the level density or the parameter α. The results agree with those obtained recently by Karrasch *et al.* [13,14] by using the renormalization group approach for $N=2$ and 4 resonance states. However, the results with random V_i^c and a larger number of resonance states show some new features. We show explicitly that Fano-like resonances may appear in the transmission under certain conditions. They differ, however, from the Fano resonances known to appear in the one-continuum case ($K=1$).

As a result of our study we relate, in Sec. IV, the uniform phase lapses observed at high level density, to the resonance trapping phenomenon characteristic of the regime of overlapping resonances. Mathematically, this phenomenon follows from the non-Hermiticity of the Hamilton operator $\widetilde{H}_{\rm eff}$ describing the open quantum system. It is linked to singular points (and their neighborhood) in the continuum at which (at least) two eigenvalues of $\widetilde{H}_{\rm eff}$ coalesce. Some conclusions are drawn in the last section. Most interesting is the relation between phase lapses and resonance trapping, on the one hand, and other experimental results being puzzling in the framework of the standard Hermitian Hamiltonian quantum physics, on the other hand.

As to the notation used in the present paper, we state the following. In scattering theory, the different continua are denoted usually by different decay channels. A two-channel case is, as a rule, an inelastic process. In the transmission, however, we have at least two channels: one channel of incoming waves and another one of outgoing waves. If the two attached leads are identical, the process is elastic in spite of the presence of (at least) two channels. Furthermore, transmission with one channel in each lead is considered often to be a one-channel process. In order to avoid confusion, we do not use the terminology *decay channel* in the present paper. Instead, we write *continuum of scattering wave functions.* It will be shown that the number K of continua is decisive for all the redistribution processes taking place in the regime of overlapping resonances. It determines therefore also the phenomenon of resonance trapping. Furthermore, the Fano-like resonances appearing in the transmission through a quantum dot with two identical attached leads (corresponding to $K=2$), are different from the Fano resonances known from scattering theory in the one-continuum case ($K=1$), as will be shown in Sec. IV A.

II. MODEL

The basic idea of the FPO method is the subdivision of the whole function space into two subspaces one of which (Q subspace) contains all wave functions that are localized inside the system and vanish exponentially outside of it while the wave functions of the other subspace (P subspace) are extended up to infinity and vanish inside the system [16]. The solutions in the two subspaces can be found by means of standard methods. In particular, it is possible to treat the many-body problem since the many-body interactions are incorporated in the Hamilton operator H_B of the Q subsystem and therefore in the solutions of

$$(H_B - E_i^B)\Phi_i^B = 0. \tag{1}$$

The eigenfunctions Φ_i^B ($i=1,\ldots,N$) of H_B are orthonormalized according to the Kronecker delta δ_{ik} and the solutions of

$(H_C-E)\xi_E^c$ in the P subspace according to the Dirac δ function $\delta(E-E')$. Here, c denotes a specific continuum of scattering wave functions, $c=1,\ldots,K$. It is $QP=PQ=0$ and $P+Q=1$, where Q and P are the projection operators to the respective subspaces.

The Schrödinger equation in the whole function space reads

$$(H-E)\Psi_E^c=0 \tag{2}$$

where $H=H_B+H_C+V_{BC}+V_{CB}$ as well as H_B and H_C are Hermitian Hamilton operators, H_B is defined in the Q subspace, H_C in the P subspace and V_{BC}, V_{CB} describe the interaction between the two subspaces. The wave functions Ψ_E^c can be found, without any approximations, by applying $P+Q=1$ to Eq. (2) and finding the expression $\Psi_E^c=P\Psi_E^c+Q\Psi_E^c$. In solving Eq. (2), the effective non-Hermitian Hamilton operator

$$\tilde{H}_{\rm eff}=H_B+\sum_c V_{BC}\frac{1}{E^+-H_C}V_{CB} \tag{3}$$

appears [23] which contains the Hamilton operator H_B of the closed (isolated) system with discrete states, see Eq. (1), as well as an additional symmetric term that describes the coupling of the discrete states via the common environment of scattering wave functions ξ_E^c. Further, V_{BC}, V_{CB} stand for the coupling between the *eigenstates* of H_B and the environment that may consist of several continua c. The operator $\tilde{H}_{\rm eff}$ describes the localized part of the problem. It is non-Hermitian and symmetric,

$$(\tilde{H}_{\rm eff}-z_i)\tilde{\Phi}_i=0;\quad \langle\tilde{\Phi}_i^*|\tilde{\Phi}_j\rangle=\delta_{ij}. \tag{4}$$

Its eigenvalues $z_i=\tilde{E}_i-i/2\tilde{\Gamma}_i$ and eigenfunctions $\tilde{\Phi}_i$ are complex. The eigenvalues provide not only the energies $\tilde{E}_i$ of the resonance states but also their widths $\tilde{\Gamma}_i$ (inverse lifetimes). The eigenfunctions are biorthogonal according to Eq. (4) with the consequence that their phases are not rigid in the regime of overlapping resonances [19–21]. The crossing points at which two (or more) eigenvalues z_i of $\tilde{H}_{\rm eff}$ coalesce, are singular points. Here, the corresponding eigenfunctions $\tilde{\Phi}_i$ become linearly dependent, $\tilde{\Phi}_1\rightarrow\pm i\tilde{\Phi}_2$.

Since $\tilde{H}_{\rm eff}$ depends explicitly on energy, so do its eigenvalues and eigenfunctions. The energy dependence of the z_i and $\tilde{\Phi}_i$ is important near decay thresholds and in the regime of overlapping resonances. The z_i and $\tilde{\Phi}_i$ describe the spectroscopic properties of the system localized in the Q subspace and embedded in the P subspace. Using the eigenvalues z_i and eigenfunctions $\tilde{\Phi}_i$ of $\tilde{H}_{\rm eff}$, the solution of Eq. (2) reads

$$\Psi_E^c=\xi_E^c+\sum_{i=1}^N \Omega_i\frac{\langle\tilde{\Phi}_i^*|V_{QP}|\xi_E^c\rangle}{E-z_i};\quad \tilde{\Omega}_i=(1+G_P^{(+)}V_{PQ})\tilde{\Phi}_i, \tag{5}$$

where $\tilde{\Omega}_i$ is the wave function of the resonance state i and $G_P^{(+)}$ is the Green's function in the P subspace. The expression (5) represents a solution of the problem (2) which is exact provided that all interactions are known analytically and $P+Q=1$ holds. For a numerical proof of this statement in the case of resonance scattering on Bargmann-type potentials see [24].

By means of the expression (5) for Ψ_E^c, the resonance part of the S matrix can be derived [16,25]

$$S_{cc'}^{\rm res}=i\sum_{i=1}^N\frac{\gamma_i^c\gamma_i^{c'}}{E-z_i}, \tag{6}$$

with $\gamma_i^c=\sqrt{2\pi}\langle\tilde{\Phi}_i^*|V_{BC}|\xi_E^c\rangle=\sqrt{2\pi}\langle\xi_E^c|V_{CB}|\tilde{\Phi}_i\rangle$ when excitation and decay of the states occur via the same mechanism. In $S_{cc'}^{\rm res}$, the eigenvalues z_i and eigenfunctions $\tilde{\Phi}_i$ of $H_{\rm eff}$ are involved. The $\gamma_i^c\gamma_i^{c'}$ show a special resonance behavior at the energy of a branch point where two eigenvalues z_i of $H_{\rm eff}$ coalesce [26]. Details of the model can be found in [16].

Using the expressions (2)–(6), numerical studies for small quantum systems such as nuclei, atoms and quantum dots are performed, see the review [16]. Of special interest are the results obtained in the regime of overlapping resonance states. They show generic features such as level repulsion and width bifurcation which are caused by the phenomenon of avoided and true crossings of resonance states in the continuum. Mathematically, they can be traced back to the nontrivial topological structure of the continuum, i.e., to the existence of singular points (exceptional points) in the continuum [19,27]. The role of these points and their neighborhood for the dynamics of open quantum systems is discussed recently in detail [16,28].

The width bifurcation appearing at comparably large coupling strength between system and environment causes the appearance of long-lived (trapped) states together with a few short-lived ones. The mechanism is the alignment of the wave functions of a few states to the scattering wave functions of the environment by trapping the rest of the states (*phenomenon of resonance trapping*). The alignment is possible due to the biorthogonality of the eigenfunctions $\tilde{\Phi}_i$ of the non-Hermitian operator $\hat{H}_{\rm eff}$ as a result of which the phase rigidity of the $\tilde{\Phi}_i$ may break down [16,19–21]. The coupling coefficients of the trapped resonance states to the continuum of scattering wave functions are correlated since $\langle\tilde{\Phi}_i|\tilde{\Phi}_{j\neq i}\rangle\neq 0$ and $\langle\tilde{\Phi}_i|\tilde{\Phi}_i\rangle>1$ in the regime of spectroscopic redistribution processes. Numerical studies for the nucleus ^{24}Mg have proven this statement [29].

Number and energy position of distant resonance states (low level density) are determined, to a good approximation, by the eigenstates of H_B (which contain the interactions between the particles of the system). Due to the spectroscopic redistribution processes taking place in the regime of overlapping resonances, number and position of the trapped resonance states (high level density) depend on the overall coupling strength between system and environment. The number of trapped resonance states is smaller than the number of eigenstates of H_B.

All calculations performed by means of the Feshbach projection operator formalism show that the number of continua of scattering wave functions plays the decisive role in the

redistribution process taking place in the regime of overlapping resonances. Whether or not also an energy loss takes place is of minor importance. The transmission process through a quantum dot with two identical attached leads (corresponding to $K=2$) shows therefore the characteristic features of a two-continua process. For example, a few resonance states align each to one of the continua such that the number of trapped resonance states is smaller than N (where N is the number of eigenstates of H_B). Mostly, the number of trapped resonance states is $N-2$. Fano-like resonances appearing in the transmission through a quantum dot without any energy loss in the dot, differ from the Fano resonances (originally defined for the one-continuum case), as will be shown in Secs. III C and IV A.

In order to show the *generic* features of open quantum systems as a function of the coupling strength between the two subspaces, the effective non-Hermitian Hamiltonian (3) can be approximated by the expression

$$H_{\mathrm{eff}} = H^0 - i\alpha VV^+, \tag{7}$$

where the first term H^0 describes the internal structure of the system in the Q subspace and αVV^+ stands for the coupling between the two subspaces (in terms of the eigenvectors of H^0). Both operators H^0 and VV^+ are Hermitian. This expression for H_{eff} is used in many model calculations in order to simulate some important features of open quantum systems at strong coupling to the continuum, see the recent review [16]. It gives however reliable results only up to values of α somewhat larger than the critical coupling strength $\alpha=\alpha_{\mathrm{cr}}$ at which K broad resonance states and $N-K$ trapped states are formed (where K is the number of continua). The expression (7) is energy independent and can describe the generic features of the system only at energies far from decay thresholds. When α is chosen to be real, the Hermitian part of the second term of Eq. (3) is effectively taken into account by considering $H_0^{\mathrm{eff}}=H^0+\Sigma_c \mathcal{P}\int dE' \frac{\gamma_i\gamma_j}{E-E'}$. Alternatively, α can be chosen to be complex. In such a case, H^0 remains unchanged and the principal value integral in H_{eff} is simulated by $\mathrm{Re}(i\alpha VV^+)$. In both cases, $\mathrm{Im}(i\alpha VV^+)$ stands for the residuum of the non-Hermitian term of H_{eff}.

In any case, the parameter α is the mean overall coupling strength between discrete and continuum states while the components V_i^c of the vectors V describe the coupling of the individual resonance states i to the continua c (in terms of the eigenvectors of H_B). The rank of H_0 is equal to the number N of states of the system, $i=1,\ldots,N$. The coupling matrix V is of rank $K\times N$ where $K<N$ is the number of continua, $c=1,\ldots,K$. Thus, the rank of VV^+ is K. Below the critical coupling strength, $\alpha<\alpha_{\mathrm{cr}}$, we have N resonance states while there are only $N-K$ narrow resonance states when $\alpha>\alpha_{\mathrm{cr}}$. The $N-K$ resonance states at $\alpha>\alpha_{\mathrm{cr}}$ and their coupling vectors to the continuum differ from those at $\alpha<\alpha_{\mathrm{cr}}$. These results are independent of the number N of states and hold also in the limit $N\to\infty$, see the analytical study [30].

It should be underlined here once more that Eq. (7) allows to describe generic features of open quantum systems that arise from the coupling of the system to the environment of scattering wave functions. The Hamiltonian (7) can, however, *not* be used for the description of all details of the system. For example, the number of short-lived whispering gallery modes which may appear under certain conditions in open quantum cavities with convex boundary is larger than K [20,31]. Also effects arising from the interaction between the particles of the system cannot be studied directly by using Eq. (7). In order to receive detailed information for the special system considered, the Hamiltonian (3) and all the related complex matrix elements have to be calculated. Furthermore, the boundary conditions have to be taken into account correctly. This leads to some restrictions in the application of the simple expression (7) as discussed above. In other words, it is possible to receive generic features of open quantum systems on the basis of Eq. (7) when the applicability of this simple formula to the description of the system is controlled by Eq. (3).

The eigenfunctions Φ_i and eigenvalues $\mathcal{E}_i=E_i-i/2\Gamma_i$ of the Hamilton operator H_{eff}, Eq. (7), are complex since H_{eff} is non-Hermitian. The eigenfunctions Φ_i are biorthogonal, $\langle\Phi_i^*|\Phi_j\rangle=\delta_{ij}$. Mathematically, the biorthogonality of the eigenfunctions of H_{eff} is basic for the dynamics of open quantum systems in the regime of overlapping resonance states. The generic features of open quantum systems are involved in Eq. (7) and can be controlled in a transparent manner.

Using the energy independent approach (7) for H_{eff}, the scattering matrix simplifies to

$$S_{ab}(E) = \delta_{ab} - 2i\alpha\sum_i \frac{W_i^a W_i^b}{E-\mathcal{E}_i}, \tag{8}$$

where a and b denote two continua of scattering wave functions and the coupling vectors W_i^a and W_i^b are written in terms of the eigenvectors in the biorthorgonal eigenbasis of H_{eff}. For trapped resonance states, we have a corresponding expression and, additionally, a background term. The partial cross section for the reaction from continuum a to continuum b is then given by

$$\sigma_{ab}(E) = |\delta_{ab} - S_{ab}(E)|^2 \tag{9}$$

with the phase

$$\varphi_{ab}(E) = \arg[S_{ab}(E)]. \tag{10}$$

According to this simple toy model, the redistribution of the spectroscopic features of the system can be controlled by varying α from zero (corresponding to the closed system with N levels) to a value at which the second term of H_{eff} dominates whose rank is $K<N$. Since the eigenfunctions of H_{eff} in the regime of the spectroscopic redistribution are biorthogonal, the coupling coefficients W_i^c of the different resonance states i to the continuum are correlated in this regime. Resonance trapping occurs hierarchically [17,20,32–34]. Finally, the widths Γ_i of only K states are large such that these states are no longer localized in the Q subspace and the simple Hamiltonian (7) does no longer describe the system. The widths Γ_i of the rest of the states are small (*resonance trapping*) [34]. That means, a dynamical phase transition

takes place [16] and, as a consequence, the system has only $N-K$ long-lived resonance states.

We are interested in the simulation of transmission through small systems coupled to two (almost) identical leads at zero temperature. The transmission is given by S_{ab} with $b \neq a$. According to $K=2$ continua in this case, two short-lived states together with $N-2$ long-lived trapped ones are formed at strong coupling. Transmission zeros may appear due to destructive interferences between the wave functions of the resonance states. At the energies of the transmission zeros, the reflection is maximal and the coupling between system and environment vanishes. These energies are therefore independent of α and are determined by H_B and H^0, respectively, and the coupling vectors V^a and V^b to the continuum. At the energies of the transmission zeros, phase lapses appear the positions of which are, consequently, also independent of α. At $\alpha \approx \alpha_{\rm cr}$ and $\alpha > \alpha_{\rm cr}$, the so-called mesoscopic properties of the resonance states known at small $\alpha < \alpha_{\rm cr}$ (low level density), are washed out.

III. NUMERICAL RESULTS

In this section, we show the results of calculations performed with Eqs. (7)–(10). In all cases, H^0 is chosen diagonal with the diagonal matrix elements E_i^0. In order to simulate the transmission through a cavity with two attached leads, we restrict ourselves to the two-continua case ($K=2$). After fixing the $N \times 2$ components of the coupling vectors V^c, $c=1,2$, we trace the eigenvalues of $H_{\rm eff}$ as a function of the coupling parameter α. We calculate the transmission probability $\sigma_{12}(E)$ and the transmission phases $\varphi_{12}(E)$ for different level densities of H^0 and distributions of the coupling vectors V^c at some selected values of the coupling strength α. Furthermore, we choose α to be real or complex with $\mathrm{Im}(\alpha)=\mathrm{Re}(\alpha)$ in the last case. In order to illustrate the resonance trapping effect, the calculations are performed by varying α from small values to $\alpha_{\rm cr}$ and further to values $\alpha > \alpha_{\rm cr}$.

A. Increasing level density and fixed coupling strength α

First, we show results obtained for $N=10$ states of H^0 with increasing level density coupled to $K=2$ continua of scattering wave functions (Fig. 1). The $N=10$ energies E_i^0 of the unperturbed states are chosen such that the distance between them is halved with increasing energy, i.e., $E_1^0=5$, $E_2^0=7.5$, $E_3^0=8.75$ and so on. The subfigures on the right-hand side of Fig. 1 are a magnification of the region with high level density.

We choose the two $N=10$ dimensional coupling vectors V^c, $c=1,2$, of the two continua as $\mathrm{sign_V}(1+\eta)$, where $\mathrm{sign_V}$ is the sign of the elements of the coupling vector and η is a Gaussian random number with zero mean and standard deviation 0.1. In Fig. 1, $\mathrm{sign_V}$ is chosen to be +1 for the first continuum and −1 for the second one. The eigenvalue trajectories are calculated by varying the value of the real and imaginary part of α between 4×10^{-3} and 2 in steps of 4×10^{-3}. The cross sections $\sigma_{12}(E)$ and the phases $\varphi_{12}(E)$ are calculated with $\alpha=(1+i)0.05$. The spectroscopic values, i.e., energy positions and decay widths of the resonance states for which cross section and phases are calculated, are marked by square symbols in the eigenvalue pictures.

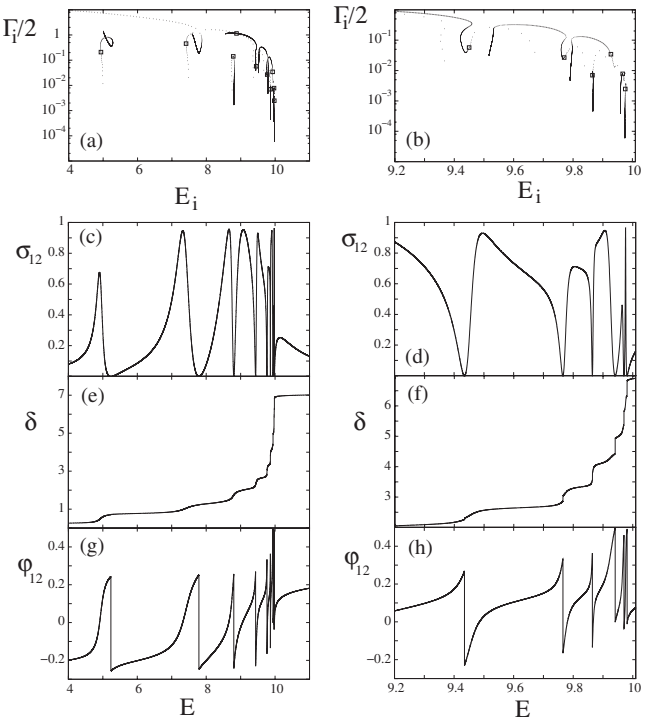

FIG. 1. (a) and (b): eigenvalue trajectories $\mathcal{E}_i=E_i-i/2\Gamma_i$ as a function of the coupling parameter α (the real energy axis is scaled according to the positions of the unperturbed states as described in the text), (c) and (d): transmission probability $|\sigma_{12}(E)|^2$ (normalized to 1), (e) and (f): scattering phase $\delta(E)$ in units of 2π, (g) and (h): phase $\varphi_{12}(E)=\arg[\sigma_{12}(E)]$ for $N=10$ states in units of 2π. The distance ΔE between every two consecutive states E_i^0 is halved successively with increasing energy. In (a) and (b), the parameter α is varied between 4×10^{-3} and 2 in steps of 4×10^{-3}. The cross sections $\sigma_{12}(E)$, the scattering phases $\delta(E)$ and the phases $\varphi_{12}(E)$ are calculated with $\alpha=(1+i)0.05$ (marked by squares in the eigenvalue trajectories). The coupling vectors are $1=v_i^{c=1}=-v_i^{c=2}$; $i=1\ldots10$. The density of points in the subfigures (a) and (b) expresses the "velocity" with which the eigenvalues $\mathcal{E}_i$ of $H_{\rm eff}$ change as a function of α. The resonance trapping occurs hierarchically. Note the different energy scales in the figures on the right-hand and left-hand side.

In the subfigures (a) and (b), we show the trajectories of the eigenvalues $\mathcal{E}_i=E_i-i/2\Gamma_i$ of $H_{\rm eff}$ as a function of the coupling parameter α. The distance between adjacent points of a given trajectory expresses the "velocity" by which the eigenvalues move in the complex plane as a function of α. The two short-lived states arise in the region of high level density and are continuously shifted to lower energy. Energy shifts to the low-energy region at large α occur also in calculations with real α though they are smaller in this case.

The eigenvalue pictures confirm the general consideration given in Sec. II and illustrate some further details of the reorganization process. At first, all eigenvalues drift from the real axis into the complex plane such that the real part, i.e., the energy position of the resonance states, remains almost unchanged. In this low coupling regime, the imaginary parts

and thus the resonance widths increase monotonically with increasing α. Thereafter, a critical regime is reached where two neighboring resonance states attract each other in energy while their widths bifurcate. This region is determined by true and avoided crossings of the eigenvalue trajectories. The true crossing points are singular points at which not only the eigenvalues of two eigenstates of Eq. (7) coincide ($\mathcal{E}_1=\mathcal{E}_2$) but also their wave functions become linear dependent from one another ($\Phi_1=\pm i\Phi_2$), for details see [16]. The avoided crossings appear in the neighborhood of singular points. This is illustrated, e.g., in Fig. 1 in [35] where the crossing points are marked on the eigenvalue trajectories, and in [36] where the eigenvalue trajectories in the neighborhood of the crossing points (*double poles of the S* matrix) in laser-induced continuum structures in atoms are shown. The calculations in the first case are performed by using Eq. (7) and those in the second case by using Eq. (3). Finally a few short-lived states appear while the remaining ones get trapped, i.e., become effectively decoupled from the continuum of scattering wave functions. In our case, we have $K=2$ short-lived states that trap the remaining $N-K=8$ states.

These spectroscopic reordering processes set in when neighboring states start to overlap. Therefore, the critical regime is reached at values α which are the smaller the larger the level density is. The reordering regime covers a finite range $\Delta\alpha$ of the parameter α since the resonance trapping phenomenon occurs hierarchically, e.g., [32]. Each of the two short-lived states is aligned to one of the two scattering wave functions while the trapped states encounter orthogonal orientations with respect to the scattering wave functions [34]. Their widths do not increase with further increasing α.

The subfigures (c) and (d) show the transmission probability σ_{12} as a function of energy for a fixed value of α. The corresponding complex eigenvalues are marked by squares in the eigenvalue trajectories of the subfigures (a) and (b). The decrease of the widths of the resonances at high level density can be seen immediately in the narrowing of the resonances.

In the subfigures (e) and (f), the scattering phases $\delta(E)$ are shown. They increase regularly by π (in accordance with the Levinson theorem) when the position of a resonance state is crossed. In the two subfigures (g) and (h), we show the phases $\varphi_{12}=\arg(S_{12})$. They jump by π or $-\pi$ at the zeros of the transmission probability σ_{12} (see Sec. III B for further discussion).

Interesting is the variation of the shape of the phases $\varphi_{12}=\arg(S_{12})$ when the level density is increased. In any case, the increase of φ_{12} occurs in the energy region $\Delta_i=E_i\pm\Gamma_i$ around the position E_i of the resonance state i while a phase lapse appears at the zero in the cross section, i.e., at an energy between two neighboring resonances. The position of a resonance state causes a peak in the cross section that is well separated from zeros if the resonances do not overlap (regime at low level density with Breit-Wigner resonances). With increasing level density, the resonance states do no longer cause peaks, but mostly dips in the cross section, and the positions of the resonance states are no longer well separated from the cross section zeros. Hence, the shape of $\varphi_{12}(E)$ changes qualitatively, compare the subfigures (g) and (h).

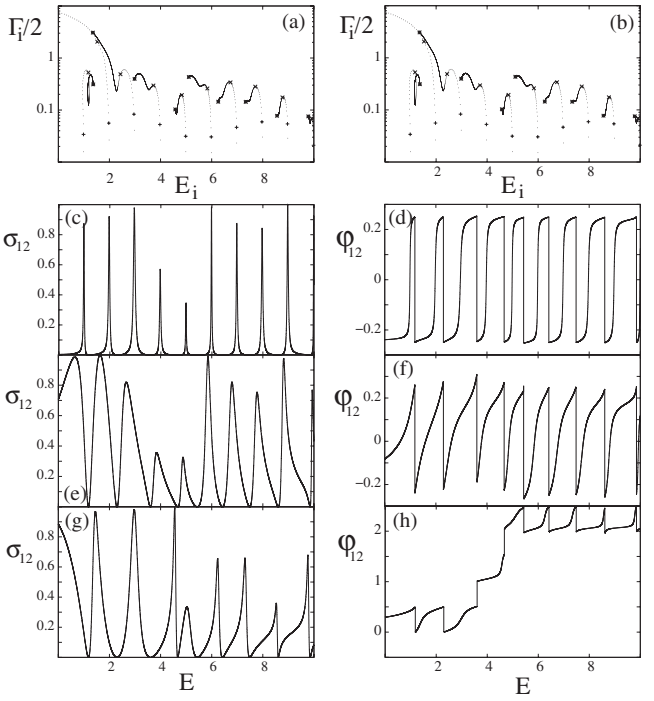

FIG. 2. (a) and (b) eigenvalue trajectories $\mathcal{E}_i=E_i-i/2\Gamma_i$ for ten equidistant states as a function of the coupling parameter α (the real energy axis is scaled according to the positions of the unperturbed states as described in the text). $\mathrm{Re}(\alpha)=\mathrm{Im}(\alpha)$ is varied from 0.005 to 2.5 in steps of 0.005. (c), (e), and (g): transmission probability $|\sigma_{12}(E)|^2$ (normalized to 1) calculated with $\mathrm{Re}(\alpha)=\mathrm{Im}(\alpha)=0.01$, 0.1 and 2.5 [marked in the subfigures (a) and (b) by +, x and $*$, respectively]. (d), (f), and (h): the corresponding phases $\varphi_{12}(E)=\arg(\sigma_{12}(E))$ in units of 2π. It is sign_V+1 for the first and -1 for the second continuum.

The results shown in Fig. 1 and those obtained for the case with $\mathrm{sign}_V=+1$ of both coupling vectors (not shown in the present paper) have the same characteristic features as those found by Karrasch *et al.* [13,14] by using the renormalization group theory for the transmission through a microwave cavity with, respectively, 2 and 4 resonance states. As our simple schematic model with the Hamilton operator H_{eff}, Eq. (7), does not contain any specific features of any particular quantum system, we consider this behavior as a generic one.

We performed also calculations with random coupling vectors (including their signs). These results (not shown) show some unique effects. Typically, the number of zeros in the cross section may be smaller than in the other two cases with regular signs of the coupling coefficients. Correspondingly, also the number of phase lapses may be reduced. That means, it does no longer hold that a transmission zero and the corresponding phase lapse occur between every two resonances.

B. Equidistant levels and increasing coupling strength α

In Fig. 2, we show the results obtained for ten equidistant levels coupled to two continua of scattering wave functions. The $N=10$ components of the coupling vectors V^c, $c=1,2$, of

the two continua are chosen as $\mathrm{sign}_V(1+\eta)$ where η is a Gaussian random number with zero mean and standard deviation 0.1. It is $\mathrm{sign}_V=+1$ for the first and -1 for the second continuum. The parameter α is complex with $\mathrm{Re}(\alpha)=\mathrm{Im}(\alpha)$. In the eigenvalue trajectories, both $\mathrm{Re}(\alpha)$ and $\mathrm{Im}(\alpha)$ are varied from 0.005 to 2.5 in steps of 0.005. The cross sections σ_{12} and the phases φ_{12} are calculated for the three values $\mathrm{Re}(\alpha)=\mathrm{Im}(\alpha)=0.01$, 0.1 and 2.5 which are marked in the subfigures (a) and (b) by, respectively, +, x and $*$. The subfigures (a) and (b) show the same data in order to relate visually the positions of the resonance states to the cross sections (left) and to the phases (right).

At small α, the resonances are well isolated and of Breit-Wigner shape. The regime with intermediate values of α is the critical one where the resonance states overlap and most of them become trapped. Characteristic of this regime is the local interplay of neighboring resonance states. Some of the states first trap other ones in the neighborhood and then become trapped by more distant ones. At large coupling strength α, all but two resonance states are trapped.

In Fig. 2, we see the same generic effects as in Fig. 1 although the level density is constant on the average in this case. The point is that the effects seen in the two figures are caused by the increasing degree of resonance overlapping which is achieved, in the first case, by increasing level density and, in the second case, by increasing overall coupling strength α. Mathematically, both situations are equivalent to one another since resonance overlapping is described, in both cases, by nonvanishing nondiagonal terms of H_{eff}. In both figures, we see phase lapses of π or $-\pi$ at the energies of the zeros of the transmission probability. Also the energy dependence of φ_{12} around the phase lapse changes in Fig. 2 in the same manner as in Fig. 1 when the degree of overlapping of the resonances is changed.

In Fig. 2, zeros in the cross section appear between every two resonances. The position of these zeros and of the corresponding phase lapses does not depend on the parameter α. The phase lapses are $-\pi$ at low and critical values of α. At large coupling strength, some of the phase lapses change their sign. The results obtained with $\mathrm{sign}_V=+1$ for both coupling vectors (not shown) display qualitatively the same characteristic features as those shown in Fig. 2.

We discuss now in detail the results obtained for ten equidistant states with random components of the coupling vectors V^c, $c=1,2$. In Figs. 3–5, the components V_i^c are chosen as Gaussian random numbers with zero mean and unit variance, see Table I. The coupling parameter α is chosen, in these calculations, to be real and complex, respectively, with $\mathrm{Im}(\alpha)=\mathrm{Re}(\alpha)$ in the last case. The corresponding eigenvalue trajectories $\mathcal{E}_i$ are shown at the top and bottom, respectively, of Fig. 3.

In the central part of Fig. 3, we show the cross sections and phase lapses at small [subfigures (c) and (d)], intermediate [subfigures (e) and (f)] and large coupling strength α [subfigures (g) and (h)]. The results with $\mathrm{Im}(\alpha)=0$ (full lines) and $\mathrm{Im}(\alpha)=\mathrm{Re}(\alpha)$ (dashed lines) are surprisingly similar although the corresponding eigenvalue pictures differ considerably from one another. The cross section obtained for the large value $\alpha=2.5$ [Fig. 3(g)] shows two resonance peaks less than that obtained with the small value $\alpha=0.01$

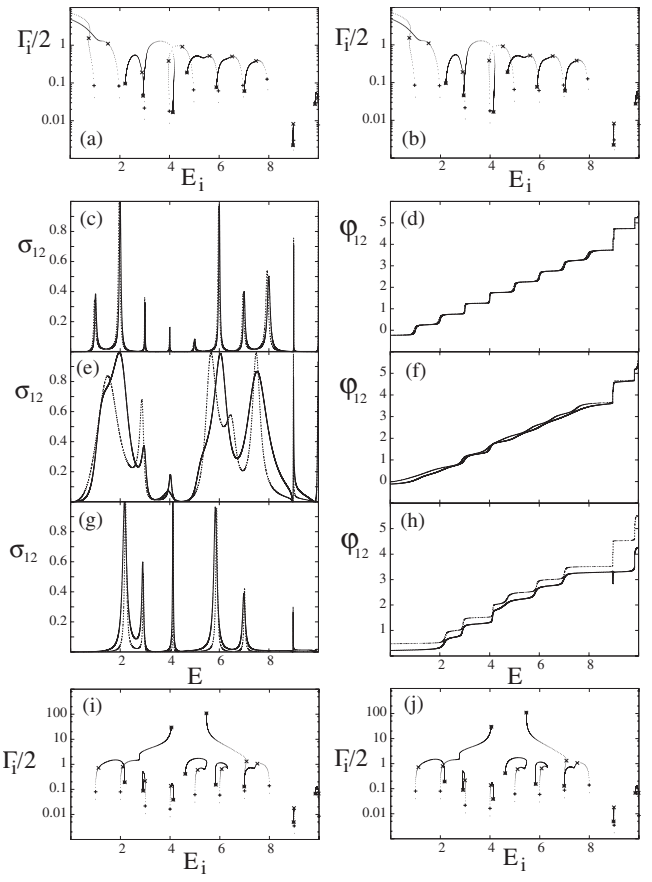

FIG. 3. The same as Fig. 2 but the coupling vectors V^c, $c=1,2$, are chosen with Gaussian random numbers with zero mean and unit variance (Table I). Full lines in (c) to (h): $\mathrm{Im}(\alpha)=0$, dashed lines: $\mathrm{Im}(\alpha)=\mathrm{Re}(\alpha)$. The subfigures (i) and (j) show the eigenvalue trajectories $\mathcal{E}_i$ with $\mathrm{Im}(\alpha)=0$.

[Fig. 3(c)]. This result corresponds to the fact that the number of long-lived resonance states is reduced at large α due to the resonance trapping phenomenon (see the eigenvalue trajectories at the top and bottom of Fig. 3). At large α two states are short-lived according to their alignment each with one of the scattering wave functions. They are not visible as resonances in the cross section but appear as a background superposing the long-lived resonance states.

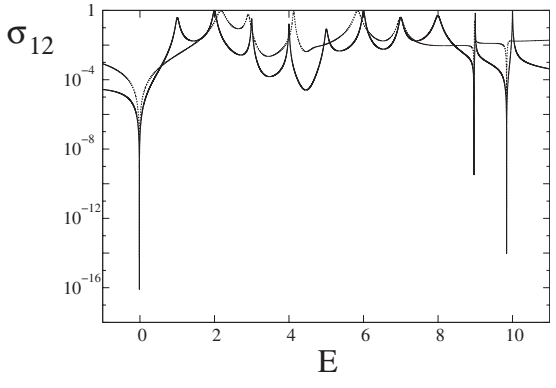

FIG. 4. Cross section σ_{12} with $\mathrm{Im}(\alpha)=0$ of Fig. 3 in logarithmic scale. Full line: small α as in Fig. 3(c), dashed line: large α as in Fig. 3(g).

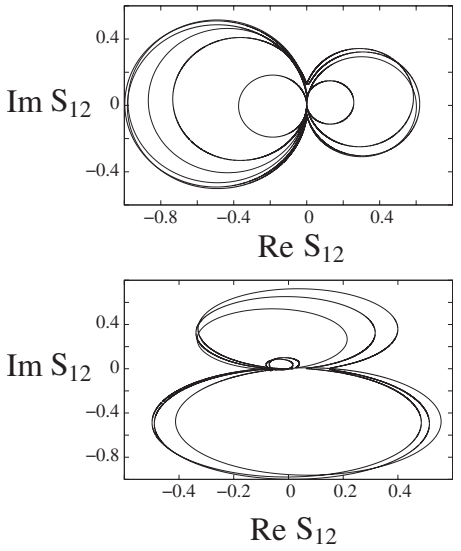

FIG. 5. The S matrix corresponding to Fig. 3 with $\mathrm{Im}(\alpha)=\mathrm{Re}(\alpha)$. Top: small α as in Fig. 3(c), bottom: large α as in Fig. 3(g).

The number of zeros in the cross section may be much smaller than the number of resonance states. It is exclusively determined by the distribution of the E_i^0 and the coupling vectors V^c. When the coupling vectors are those given in Table I, there are only three zeros for ten resonance states coupled to two continua, This can clearly be seen in Fig. 4 where the cross section is shown in logarithmic scale for small (full line) and large (dashed line) value of α [with $\mathrm{Im}(\alpha)=0$].

Phase lapses appear at every zero in the cross section as can be seen from Fig. 3 right hand. They are $\pm\pi$.

For illustration, we show in Fig. 5 the S matrix for small (top) and large (bottom) coupling strength α. In this calculation, α is complex with $\mathrm{Im}(\alpha)=\mathrm{Re}(\alpha)$. We see the rotation of the S matrix that takes place in the transition from the weak coupling regime (top, small α) to the strong one (bottom, large α). It illustrates the alignment of the resonance states with the scattering states of the continuum [16,19]. The transition through zero is mostly avoided at both small and large coupling strength α such that, in the present case, the zero is passed only three times according to the three zeros in the cross section.

TABLE I. The coupling vectors V_i^c used in Fig. 3.

State i	Continuum $c=1$	Continuum $c=2$
1	1.887	−0.658
2	−1.370	−1.456
3	−0.322	0.992
4	−0.882	−0.187
5	1.741	−0.255
6	−1.312	−1.126
7	1.950	−0.704
8	−2.450	−1.004
9	−0.359	−0.200
10	−0.424	−0.491

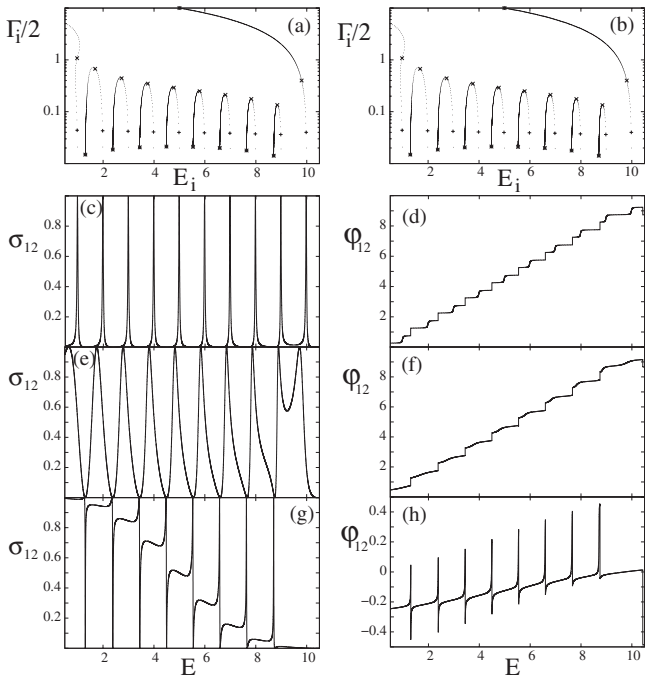

FIG. 6. The same as Fig. 2 but the components of the first coupling vector are chosen as +1, the last component of the second coupling vector as −1 and the rest of the components as +1. In (a) and (b), $\mathrm{Re}(\alpha)=\mathrm{Im}(\alpha)$ is varied between 0.005 and 2.5 in steps of 0.005. It is $\alpha=0.01$ in (c) and (d), $\alpha=0.1$ in (e) and (f), $\alpha=2.5$ in (g) and (h).

C. Fano-like resonances in the transmission probability

We now discuss in more detail the question whether Fano resonances appear in the transmission probability calculated in the formalism used in the present paper, Eqs. (7)–(10). For this purpose, we show in Figs. 6–8 the formation of the two short-lived states at large α and their influence on cross section and phase lapses when the coupling vectors are chosen in the following manner. In the three figures, all components of the first coupling vector are chosen as +1. In Fig. 6 (with complex α) and Fig. 8 (with real α), the last component of the second coupling vector is −1 and the rest of the components is equal to +1. In Fig. 7, however, the first component of the second coupling vector is −1 and the rest of the components is equal to +1. In all cases, two broad states are formed at large α due to the resonance trapping phenomenon.

In Fig. 6, the state with the larger width arises from the state $i=1$ with coupling matrix elements (1,1) and the other one from $i=10$ with coupling matrix elements (1,−1). In Fig. 7, the two states arise from the state $i=1$ with coupling matrix elements (1,−1) and from $i=2$ with coupling matrix elements (1,1). In both cases, the state with the largest width is related to a state with the coupling matrix elements (1,1), i.e., to a state with the same sign of both coupling vectors. The state with the second largest width has the coupling matrix elements (1,−1). Also in Fig. 7, the state (1,1) is shifted, at

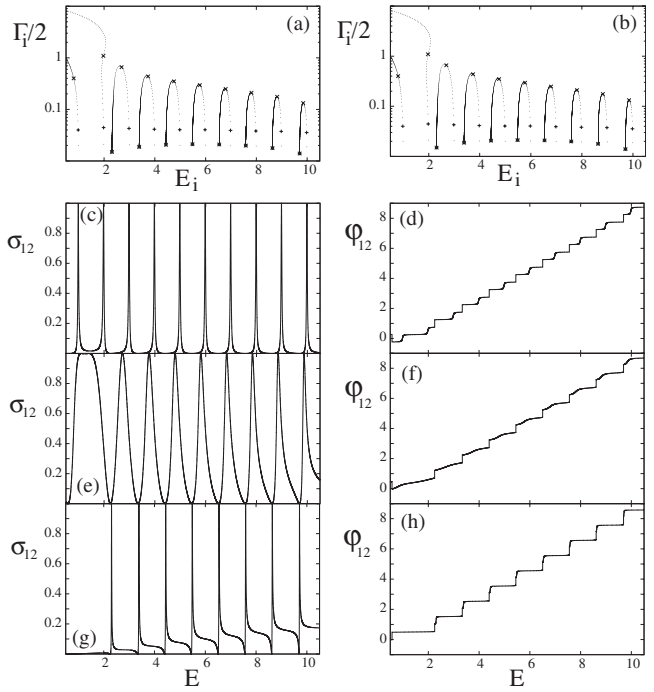

FIG. 7. The same as Fig. 6 but the first component of the second coupling vector is chosen as −1 and the rest of the components as +1.

large α, to lower energy than the state with $(1,-1)$. The two short-lived states interfere with one another such that the average cross section decreases with energy in the whole energy range shown in Fig. 6, while it increases with energy in Fig. 7 in the same energy range. The narrow resonances look like Fano resonances with a finite angle between resonance and background. This angle is different in Fig. 7 from that in Fig. 6. Correspondingly, the phase lapses have different signs in the two cases.

It should be remarked that the results shown in Fig. 6 do not depend on the fact that α is chosen to be complex in these calculations and $\mathrm{Re}(\alpha)=\mathrm{Im}(\alpha)$. Qualitatively, the same result is obtained for real α as shown in Fig. 8. Furthermore, the result shown in Fig. 6 differs from that in Fig. 7 obtained with slightly changed coupling vectors, although the results in both figures are obtained with complex α. That means, the Fano-like resonances in the two-continua case (Figs. 6–8) are different from those in the one-continuum case. In the last case, the angle of the long-lived resonance state relative to that of the short-lived state is well defined by the position of the two resonance states relative to one another (see Sec. IV A). In the two-continuum case, however, such a simple relation does not hold. As can be seen from Figs. 6–8, most important for the interference angle between narrow and broad states in the two-continuum case are the coupling vectors and not the position of the interfering states relative to one another.

All phase lapses in the three Figs. 6–8 are π at small and intermediate values of α. The difference between the two cases with complex α (Figs. 6 and 7) at large coupling strength is the angle between the short-lived and long-lived states. Correspondingly, the phase lapses are π in the one case and $-\pi$ in the other case. That means, the sign of the phase lapses is influenced by the coupling vectors. It is, however, almost independent of the fact whether α is complex or real (Figs. 6 and 8).

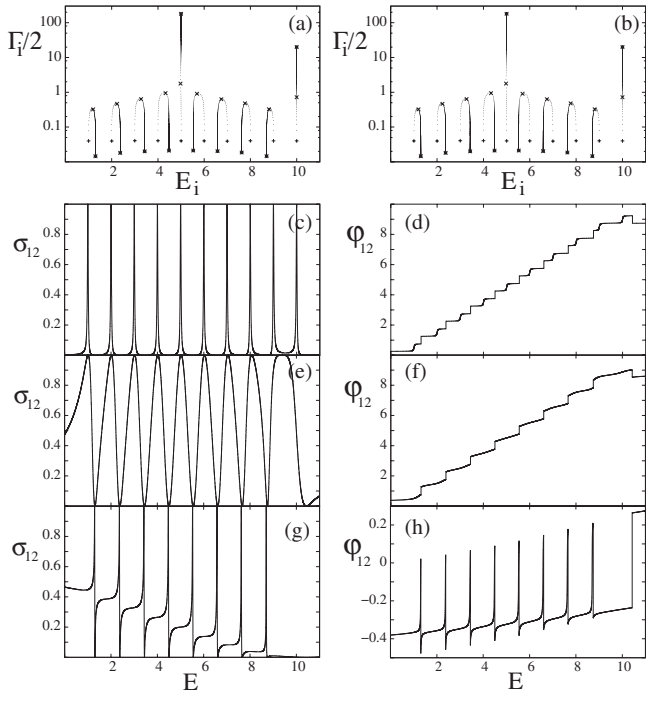

FIG. 8. The same as Fig. 6 but $\mathrm{Im}(\alpha)=0$. In (a) and (b), α is varied between 0.01 and 5.0 in steps of 0.01. It is $\alpha=0.01$ in (c) and (d), $\alpha=0.18$ in (e) and (f), $\alpha=5.0$ in (g) and (h).

IV. DISCUSSION OF THE RESULTS

The numerical results shown in Sec. III illustrate some generic features of small open quantum systems coupled to two continua of scattering wave functions. Figures 1–3 show, under different conditions, probability and phase of the transmission through a quantum dot as a function of the coupling parameter α as well as the corresponding trajectories of the eigenvalues of H_{eff}. From Fig. 4, we see that the positions of transmission zeros are independent of α, indeed.

Mathematically, the numerical results can be traced back to the loss of the phase rigidity of the eigenfunctions of the non-Hermitian Hamilton operator H_{eff} in the regime of overlapping resonances. The nonrigidity of the phases of the eigenfunctions is illustrated in Fig. 5. In Figs. 6–8, we illustrate that Fano-like resonances in the two-continua case $(K=2)$ may appear, but they differ from Fano resonances observed in the one-continuum case $(K=1)$.

In the following, we will relate the results obtained, above all, to the appearance of phase lapses in the transmission through small quantum dots and to Fano resonances. We consider also the link to other phenomena that are directly related to the resonance trapping phenomenon, e.g., to bound states in the continuum and to plateaus in the transmission probability occurring in the regime of overlapping resonances. As a remark, the calculations in Sec. III, are performed by varying α from small values up to $\alpha > \alpha_{\mathrm{cr}}$. The results for $\alpha \gg \alpha_{\mathrm{cr}}$ have illustrative character.

A. Fano resonances

Phase lapses are often related to Fano resonances [7] which have been studied originally in the one-continuum case [37]. These resonances appear in the cross section due to the interference of a narrow resonance (*the Fano resonance*) with some background that is (almost) independent of energy in the energy region $E_i-\Gamma_i \leq E \leq E_i+\Gamma_i$ (where E_i and Γ_i are energy and width of the narrow resonance). The background may arise from a state whose width is much larger than that of the narrow resonance state. The typical picture is an interference zero in the cross section in the very neighborhood of the resonance peak. The position of the zero in energy relative to that of the peak of the resonance state depends on the angle ϕ_F between resonance state and background. At $\phi_F=\pi/2$, the Fano resonance appears as a dip in the cross section such that the position of the zero of the cross section and that of the resonance state coincide. Examples for different angles ϕ_F are given in textbooks, e.g., [38]. An illustrative example is the change of the line profile of Rydberg autoionizing states due to the overlapping with a broad resonance in argon [39]. The line shape as a function of the angle between two resonance states and background is schematically considered in [40].

For the description of the transmission through quantum dots, (at least) two spatially separated continua of scattering wave functions are required. According to the S matrix theory for the transmission through quantum billiards in tight-binding approach, *two* short-lived broad states are formed at strong coupling between billiard and attached leads [41].

The numerical results for $\alpha > \alpha_{\rm cr}$ presented in Figs. 6–8 may be considered as results for eight equidistant trapped resonance states with equal coupling coefficients. They are superimposed on a background. Common to the resonances and zeros observed in the transmission and the Fano resonances (in the one-continuum case) is that both result from interference processes. However, the interference picture is, generally, more complicated and richer in the two-continua case than that in the one-continuum case. For example, the angle between narrow resonance and background in the two-continua case cannot be defined in such a simple manner as in the one-continuum case. This can be seen very clearly from Figs. 6–8: the angle is almost the same for all the narrow states in each of the figures although the position of the narrow states relative to that of the broadest state is different. In Figs. 8(g) and 8(h), the broadest state is in the center of the spectrum. However, the line shape of the low-lying and high-lying resonances is the same, in contrast to that what is known from the one-channel case (see, e.g., the line profile of Rydberg autoionizing states [39]).

B. Bound states in the continuum

The appearance of bound states in the continuum is a generic phenomenon discussed first about 80 years ago [38,42]. The mechanism is the strong parameter dependence of the decay widths due to width bifurcation (resonance trapping) as shown in different papers, see [16]. Width bifurcation is (in a similar manner as level repulsion) caused by the avoided crossing of the trajectories of the eigenvalues z_i of $\widetilde{H}_{\rm eff}$, occurring in the neighborhood of singular points in the continuum (branch points). The topological structure of the singular (crossing) points is nontrivial. Other examples of bound states in the continuum are found in laser-induced structures in atoms (so-called population trapping) [36], in photonics [43], in mesoscopic systems [44,45] and, e.g., in Aharonov-Bohm rings [46].

In [44], the FPO formalism has been applied to the transmission through double quantum dots by using the S matrix formalism together with the tight-binding approach. The trajectories of the eigenvalues of $\widetilde{H}_{\rm eff}$ as well as the transmission are controlled by an external parameter X. The trajectories $\mathrm{Im}[z_i(X)]=-2\Gamma_i(X)$ depend sensitively on X. Due to this strong parameter dependence, the unitarity of the S matrix is guaranteed at all parameter values. Furthermore, the width Γ_i of one of the states may vanish at the critical value $X=X_{\rm cr}$ if the system is symmetric in space, or may become very small if the space symmetry is somewhat broken. In the first case, a bound state in the continuum with $\Gamma_i=0$ appears.

At the positions of bound states in the continuum, phase jumps by π appear. These phase jumps differ however from the phase lapses discussed in Sec. III. They arise from the scattering phase $\delta(E)$ which jumps by π when $\Gamma_i \to 0$. An example of this type of phase lapse is shown in [44], Fig. 5, for the transmission through a double quantum dot.

The conclusion following immediately from the eigenvalue trajectories shown in Figs. 1–8, is that the zeros of the transmission probability are not caused by bound states in the continuum. Though the widths of the trapped states are small, they are different from zero in all cases considered in the present paper.

C. Brachistochrone problem

In [20,21], the transmission through small quantum dots is considered in the regime of overlapping resonances. As a result, the transmission does not show individual peaks in this regime. It is rather characterized by some "plateaus" in which some long-lived resonance states may appear as dips. One example are quantum billiards with convex boundary to which the leads are attached in such a manner that whispering gallery modes are supported [20,31]. Another example is the transition from the weak coupling to the strong coupling regime where transmission and phase rigidity are correlated and the transmission is enhanced [20,21].

These results show the characteristic features of the resonance trapping phenomenon in the two-continua case. Obviously, the system tries to find the most efficient way to connect the two continua of scattering wave functions, i.e., to solve the brachistochrone problem [16,19]. This happens in the following manner. Two different short-lived states align with the two scattering wave functions in an energy region in which the transmission probability does not vanish. The spectroscopic redistribution takes place in such a manner that a plateau appears in the transmission probability instead of two single resonance peaks. As a consequence, the transmission probability connecting the two continua of scattering wave functions is enhanced and the transmission process is

accelerated. The correlation between phase rigidity and transmission through quantum dots in the regime of overlapping resonances [20,21] supports this interpretation.

Some local plateaulike structures in the transmission probability can be seen also in the toy-model calculations of the present paper, see Fig. 7(e) around $E \approx 1$ and Fig. 8(e) around $E \approx 9.5$. In these schematical calculations, they appear instead of zeros and are not related to any phase lapses. However, they are related to the reduced phase rigidity of the resonance states in the regime of overlapping also in this case.

D. Zeros in the transmission probability and phase lapses

An analysis of scattering phases in quantum dots is performed on the basis of lattice models by Yeyati and Büttiker [5]. As a result of this study, abrupt jumps of π in the phase of the transmission amplitude are shown to be associated with the occurrence of transmission zeros and, further, the zeros of the transmission are characteristic of the isolated dot structure. They do not depend on the strength of the coupling to the leads.

These results are in agreement with those shown in Sec. III. The relation of the phase lapses to the zeros of the transmission probability follows from the S matrix. The independence of the transmission zeros of α can be seen best in Fig. 4. At energies where the transmission probability gets zero, the whole scattering process occurs via reflection. That means, at these specific energies the incoming flux is completely reflected and the coupling strength α between system and continuum does not play any role at this energy.

Consequently, number and location of the transmission zeros, and also number and location of the phase lapses, are determined exclusively by the distribution of the unperturbed levels E_i^0 (eigenstates of H^0) and the matrix elements V_i^c that characterize their coupling to the continua c. They are independent of the coupling strength α. Only the energy dependence of the phase φ_{12} in the neighborhood of the phase lapse depends on the degree of overlapping (and on α, respectively).

E. Resonance states at small and large coupling strength α

The S matrix (8) contains the coupling matrix elements W_i^a and W_i^b in terms of the eigenvectors of H_{eff}. These coupling matrix elements depend on α. Therefore also number and location of the peaks of the transmission probability depend on α. At small α, the number of peaks is equal to the number N of resonance states. At large α, the number of peaks is reduced to $N-K$, i.e., it is reduced by the number K of continua of scattering wave functions to each of which one of the K short-lived states is aligned (*resonance trapping* caused by width bifurcation). These broad short-lived states appear as background on which the $N-K$ long-lived trapped resonance states are superimposed. The energy shifts of the resonance states as a function of α and the reduction of their number by $K=2$ at large α can be seen in all our eigenvalue trajectories (Figs. 2, 3, and 6–8).

Trapping of the individual resonance states depends on the overall coupling strength α and on the local distribution of the E_i^0 as well as on the coupling vectors V^c: the values of the ith components of V determine whether the state i traps the neighboring state j (if $\Gamma_j < \Gamma_i$) or will be trapped by it (if $\Gamma_j > \Gamma_i$).

The nearest-neighbor spacing distribution of the long-lived trapped resonance states at large α differs from that of the individual resonance states at small α. This has been shown in [47] by using the non-Hermitian Hamiltonian (7) with real α. As a result of this study, even when the E_i^0 are randomly chosen according to a Poissonian distribution, the trapped resonance states at large α tend to show level repulsion similar to that of the Gaussian orthogonal ensemble (GOE). This tendency gets the more pronounced, the larger the number of continua is. Taking into account an imaginary part of α in the Hamiltonian (7) [corresponding to the principal value integral in Eq. (3)] would amplify the effect. This is due to the well-known fact that any perturbation of a Poissonian distribution by a Hermitian interaction term in the Hamilton operator induces level repulsion in the system [48]. Thus, the distribution of the resonance states at large α tends to be more uniform than the corresponding one at small α. In other words, the mesoscopic properties of the resonance states at small α are lost at large α. In order to be closer to the experimental results, the notion small (large) α used in this section, may be replaced by low (high) level density, see Sec. III B.

F. Regular features at high level density

The results discussed above (Secs. IV D and IV E) show the following features:

(i) number and position of the phase lapses *do not depend* on α,

(ii) number and position of the resonance peaks *do depend* on α.

The first feature follows from the relation of the phase lapses to the transmission zeros and the fact that the coupling between system and environment does not play any role at the position of a transmission zero. The second feature follows from the resonance trapping phenomenon appearing in the regime of overlapping resonances. It corresponds to the existence of a dynamical phase transition [16].

As a consequence of these two features, regular features in the appearance of phase lapses at high level density can be caused *only* by the changes in number and position of the narrow resonance states occurring with increasing α. Such changes are caused by the spectroscopic redistribution processes (resonance trapping) arising in the regime of overlapping resonance states. These processes cannot be traced analytically due to their relation to the singular crossing points of eigenvalue trajectories at which resonance trapping (width bifurcation) originates. The trapped resonance states are more uniform distributed than the original resonance states as calculations on the basis of the toy model (7) have shown [47], see Sec. IV E.

The results for the appearance of Fano-like resonances shown in the subfigures (g) and (h) of Figs. 6–8, may be considered as the results for eight equidistant trapped resonance states with (almost) equal coupling coefficients. In re-

alistic cases, the trapped resonance states are, of course, neither completely equidistant nor do they all have the same coupling coefficients. The results obtained represent an idealized situation which is however not far from the realistic situation in the regime with trapped resonance states. They show clearly that the Fano-like resonances appearing in the two-continua case differ from the well-known Fano resonances in the one-continuum case. They agree qualitatively with the experimental results.

We underline here the following: the coupling strength α simulates, on the one hand, the degree of opening of the system and, on the other hand, the degree of overlapping of the resonance states. Controlling an open quantum system by means of α allows therefore to obtain unambiguous information on the influence of the environment (continuum) onto the system and on the resonance trapping phenomenon induced by it. Particularly with regard to the experimentally observed regular behavior at high level density, such a study is expected to provide clear results that allow an unambiguous interpretation.

G. Comparison with other calculations

Some of the results discussed above agree with results obtained in other theoretical studies based on other methods. For example, the relation between phase lapses and zeros in the transmission probability as well as their independence of the coupling strength have been discussed in [5].

In [4], it is shown that the transmission amplitude may vanish generically in quasi-one-dimensional (quasi-1D) systems only if time reversal symmetry holds. These results are confirmed in [41,44,45] by using the tight-binding approach, but they hold only in the case of 1D systems. Generally, the existence of transmission zeros is related to that of singular points in the continuum [41]. Also in the case with time symmetry breaking, singular points exist [49]. That means, the numerical results given in Sec. III are applicable to two-dimensional (2D) and three-dimensional (3D) systems with and without symmetry breaking.

Interesting results are obtained by Oreg [12] by using a noninteracting toy model consisting of a ladder of narrow levels and a wide level. In this model, interferences between the nonresonant level and the narrow ones lead to universal phase lapses. The results are similar to ours in the regime of strongly overlapping resonances. However, the existence of a wide nonresonant level is not inherent in the model used in [12]. Instead, it is assumed to exist. This is, of course, in contrast to our studies where wide levels are shown to be formed generically at high level density (or strong-coupling strength α) due to width bifurcation.

Our results agree qualitatively with those obtained by Karrasch *et al.* for four resonance states [13] by using the numerical and functional renormalization group approaches. In [13], the results are shown as a function of V_g/Γ (where V_g is the plunger gate voltage and Γ the average coupling strength). This corresponds, qualitatively, to a representation of our results as a function of E/α (instead of E). The cross section as well as the phase lapses seem therefore to be more regular at large level density than at small one in [13]. The experimental data are represented as a function of V_g at low and high level density [3].

The results for $N=4$ resonance states obtained by Karrasch *et al.* [13] and those for $N=10$ states in our calculations agree, above all, in the fact that the widths of two resonance states are much larger than those of the rest of $N-2$ states at large resonance overlapping. This result follows from the resonance trapping phenomenon as discussed above.

V. CONCLUSION

In the present paper, transmission through systems with $N=10$ resonance states coupled to $K=2$ continua of scattering wave functions is studied in the toy model defined by Eqs. (7) and (8). The S matrix contains the eigenvalues and eigenfunctions of the non-Hermitian Hamilton operator H_{eff} that describes generic features of open quantum systems coupled to the continuum of scattering wave functions (for details see [16]). The coupling strength between states and continua can be controlled by means of the parameter α.

The transmission probability is determined by interferences between the individual resonance states. In the regime of overlapping resonance states, width bifurcation causes the appearance of $K=2$ short-lived states together with $N-K=8$ long-lived ones. The two short-lived states are aligned each with one of the continua of scattering wave functions. As a result, they cease to be localized at $\alpha \gg \alpha_{\mathrm{cr}}$. The long-lived states are trapped, i.e., they are almost decoupled from the continuum of scattering wave functions. They are well separated from one another and their wave functions are localized (in the short-time scale). Nevertheless, they differ from the individual resonance states at low level density.

The transmission probability may or may not vanish between consecutive resonance states. The position of the zeros in the transmission probability is determined by the properties of the closed system (described by the Hermitian Hamilton operator H^0) and the coupling vectors V^c of its states to the continua of scattering wave functions. It is independent of the overall coupling strength α. At the energies at which the transmission probability vanishes, phase lapses appear. Their number and locations are, therefore, also independent of α.

Number and position of peaks in the cross section depend, however, on α due to the resonance trapping phenomenon occurring in the regime of overlapping resonances around the critical value of α. The narrow trapped resonance states at high level density are distributed more regularly than the individual resonance states at low level density. The so-called mesoscopic behavior of the resonance states at low level density is lost at high level density. Hence, the probability for the occurrence of universal phase lapses between every two peaks is larger at high level density (large average coupling strength α) than at low level density (small α). These results are generic and do not depend on the particular type of interaction between the particles. They appear in calculations for concrete realistic systems with account of many-body forces [16] as well as in calculations on the basis of the toy model (7) and (8).

The variable characterizing the resonance trapping phenomenon is the number K of different scattering wave func-

tions to which the system is coupled. Thereby it is of no relevance whether or not an energy loss appears. The transmission process is (at least) a two-continua process also when it is elastic. The number of trapped (narrow) resonance states superimposed on a background at strong coupling between system and environment, is $N-K$. The $N-2$ narrow Fano-like resonances that may appear when $K=2$, differ from the Fano resonances in one-continuum case of the scattering theory: the angle between resonances and background is more complicated in the two-continua case than in the one-continuum case.

Summarizing the results of the present study, we state that the appearance of phase lapses may be related to the well-known resonance trapping phenomenon in the regime of overlapping resonances. According to this statement, the phase lapses are environmentally induced. Mathematically, environmentally induced effects (and resonance trapping) are related to the biorthogonality of the eigenfunctions of the non-Hermitian Hamilton operator H_{eff} and $\tilde{H}_{\text{eff}}$, respectively, that describes the open quantum system. As a consequence of the biorthogonality, the phases of the eigenfunctions of the Hamiltonian are not rigid: in approaching a singular point at which the eigenvalues of two resonance states coalesce, the corresponding eigenfunctions become linearly dependent. The singular points are of measure zero. However, the phase rigidity is reduced in a comparably large parameter range what leads to measurable effects in the regime of overlapping resonances [16]. A convincing explanation of phase lapses on the basis of conventional (standard) Hermitian quantum mechanics with rigid phases of the wave functions seems therefore to be impossible. Indeed, an interpolation procedure between the two limiting cases with isolated resonances at low level density and narrow resonances at high level density is introduced in [50] in order to describe the intensity pattern in an open cavity. According to the results presented in this paper, the phase lapses are generic (directly linked to singular points in the continuum). They are related therefore also to other "puzzling" results observed experimentally.

In order to prove experimentally the results obtained in the present paper, the phase lapses should be studied as a function of the degree of opening of the quantum dot, i.e., as a function of the overall coupling strength α. The advantage of such a study is that the number of states of the closed (isolated) system (described by H_B or H^0) and their coupling matrix elements V_i^c to the continuum are fixed such that the observed results can clearly be related to the phenomenon of resonance trapping. Under this condition, it should be possible to study the influence of the overlapping of the resonance states onto the spectroscopic properties of an open quantum system in a definite manner. It contains the feedback from the environment of scattering wave functions onto the system.

The results of such experimental and theoretical studies on phase lapses in concrete systems will contribute to find an answer also to other problems raised by unexpected (and often counterintuitive) experimental results on quantum dots. It is interesting to remark that an environmentally induced dynamical phase transition is recently observed in experimental and theoretical quantum chemistry studies [22]. Both phenomena are related to one another [16]. They show that the feedback between environment and system can generally not be neglected. Another question related to the same phenomenon, is whether or not bound states in the continuum exist in small quantum systems such as quantum dots (see Sec. IV B). They cause an unexpected high stability of quantum systems at certain values of external parameters. Another problem are the many experimental data on dephasing which are summarized in, e.g., [51,52], see also [16]. A quantitative description of these data by using the theory of open quantum systems with the non-Hermitian Hamilton operator $\tilde{H}_{\text{eff}}$, is not performed up to now.

All these questions are related to one another. They are of fundamental interest and may be important for applications as well. They need to be studied theoretically as well as experimentally in detail for concrete small quantum systems.

ACKNOWLEDGMENT

We thank the Max Planck Institute for the Physics of Complex Systems for hospitality.

[1] A. Yacoby, M. Heiblum, D. Mahalu, and H. Shtrikman, Phys. Rev. Lett. **74**, 4047 (1995).
[2] R. Schuster, E. Buks, M. Heiblum, D. Mahalu, V. Umansky, and H. Shtrikman, Nature (London) **385**, 417 (1997).
[3] M. Avinun-Kalish, M. Heiblum, O. Zarchin, D. Mahalu, and V. Umansky, Nature (London) **436**, 529 (2005).
[4] H. W. Lee, Phys. Rev. Lett. **82**, 2358 (1999); H. W. Lee and C. S. Kim, Phys. Rev. B **63**, 075306 (2001).
[5] A. Levy Yeyati and M. Büttiker, Phys. Rev. B **62**, 7307 (2000).
[6] Y. Oreg and Y. Gefen, Phys. Rev. B **55**, 13726 (1997); A. Silva, Y. Oreg, and Y. Gefen, *ibid.* **66**, 195316 (2002); J. König and Y. Gefen, *ibid.* **71**, 201308(R) (2005); M. Sindel, A. Silva, Y. Oreg, and J. von Delft, *ibid.* **72**, 125316 (2005); D. I. Golosov and Y. Gefen, *ibid.* **74**, 205316 (2006); New J. Phys. **9**, 120 (2007).
[7] P. G. Silvestrov and Y. Imry, Phys. Rev. Lett. **85**, 2565 (2000); Phys. Rev. B **65**, 035309 (2001); New J. Phys. **9**, 125 (2007).
[8] G. Hackenbroich, Phys. Rep. **343**, 463 (2001).
[9] V. Meden and F. Marquardt, Phys. Rev. Lett. **96**, 146801 (2006).
[10] R. Berkovits, F. von Oppen, and J. W. Kantelhardt, Europhys. Lett. **68**, 699 (2004); M. Goldstein and R. Berkovits, New J. Phys. **9**, 118 (2007).
[11] V. Kashcheyevs, A. Schiller, A. Aharony, and O. Entin-Wohlman, Phys. Rev. B **75**, 115313 (2007).
[12] Y. Oreg, New J. Phys. **9**, 122 (2007).
[13] C. Karrasch, T. Hecht, A. Weichselbaum, Y. Oreg, J. von Delft,

and V. Meden, Phys. Rev. Lett. **98**, 186802 (2007).
[14] C. Karrasch, T. Hecht, A. Weichselbaum, J. von Delft, Y. Oreg, and V. Meden, New J. Phys. **9**, 123 (2007).
[15] S. A. Gurvitz, Phys. Rev. B **77**, 201302(R) (2008).
[16] I. Rotter, J. Phys. A **42**, 153001 (2009).
[17] E. Persson, I. Rotter, H. J. Stöckmann, and M. Barth, Phys. Rev. Lett. **85**, 2478 (2000).
[18] H. Feshbach, Ann. Phys. (N.Y.) **5**, 357 (1958); **19**, 287 (1962).
[19] I. Rotter, J. Phys. A **40**, 14515 (2007).
[20] E. N. Bulgakov, I. Rotter, and A. F. Sadreev, Phys. Rev. B **76**, 214302 (2007).
[21] E. N. Bulgakov, I. Rotter, and A. F. Sadreev, Phys. Rev. E **74**, 056204 (2006).
[22] G. A. Alvarez, E. P. Danieli, P. R. Levstein, and H. M. Pastawski, J. Chem. Phys. **124**, 194507 (2006).
[23] In calculations based on statistical approaches for the eigenstates of H_B and the coupling vectors V_{BC}, V_{CB} in $\tilde{H}_{\text{eff}}$, the non-Hermiticity of $\tilde{H}_{\text{eff}}$ is usually either small or simulated by an overall imaginary part by hand. In contrast to these approaches, the non-Hermiticity of $\tilde{H}_{\text{eff}}$ in Eq. (3) follows from calculations performed for the *eigenstates* of H_B and their coupling vectors to the continuum of scattering wave functions, see [16]. In these calculations, the interaction between the particles is taken into account. As a result, the non-Hermiticity of $\tilde{H}_{\text{eff}}$ in Eq. (3) may be large, above all in the neighborhood of singularities. These singular points are crossing points of eigenvalue trajectories at which the corresponding eigenfunctions are linearly dependent. In the regime of overlapping resonances, the non-Hermiticity of $\tilde{H}_{\text{eff}}$ determines the spectroscopic redistribution processes (phenomenon of resonance trapping) and therewith the dynamics of the system.
[24] V. V. Shamshutdinova, K. N. Pichugin, I. Rotter, and B. F. Samsonov, Phys. Rev. A **78**, 062712 (2008).
[25] I. Rotter, Ann. Phys. (Leipzig) **493**, 221 (1981).
[26] I. Rotter, Phys. Rev. E **68**, 016211 (2003).
[27] U. Günther, I. Rotter, and B. F. Samsonov, J. Phys. A **40**, 8815 (2007).
[28] M. Müller and I. Rotter, J. Phys. A **41**, 244018 (2008).
[29] S. Drozdz, J. Okolowicz, M. Ploszajczak, and I. Rotter, Phys. Rev. C **62**, 024313 (2000).
[30] C. Jung, M. Müller, and I. Rotter, Phys. Rev. E **60**, 114 (1999).
[31] R. G. Nazmitdinov, K. N. Pichugin, I. Rotter, and P. Seba, Phys. Rev. E **64**, 056214 (2001); Phys. Rev. B **66**, 085322 (2002).
[32] W. Iskra, I. Rotter, and F. M. Dittes, Phys. Rev. C **47**, 1086 (1993).
[33] E. Persson, K. Pichugin, I. Rotter, and P. Seba, Phys. Rev. E **58**, 8001 (1998); P. Seba, I. Rotter, M. Müller, E. Persson, and K. Pichugin, *ibid.* **61**, 66 (2000); I. Rotter, E. Persson, K. Pichugin, and P. Seba, *ibid.* **62**, 450 (2000).
[34] M. Müller, F.-M. Dittes, W. Iskra, and I. Rotter, Phys. Rev. E **52**, 5961 (1995).
[35] W. D. Heiss, M. Müller, and I. Rotter, Phys. Rev. E **58**, 2894 (1998).
[36] A. I. Magunov, I. Rotter and S. I. Strakhova, J. Phys. B **32**, 1669 (1999); J. Phys. B **34**, 29 (2001).
[37] U. Fano, Phys. Rev. **124**, 1866 (1961).
[38] H. Friedrich, *Theoretical Atomic Physics* (Springer-Verlag, Berlin Heidelberg, 1990).
[39] A. I. Magunov, I. Rotter, and S. I. Strakhova, J. Phys. B **36**, L401 (2003).
[40] A. I. Magunov, I. Rotter, and S. I. Strakhova, Phys. Rev. B **68**, 245305 (2003).
[41] A. F. Sadreev and I. Rotter, J. Phys. A **36**, 11413 (2003); **38**, 10647 (2005).
[42] J. von Neumann and E. Wigner, Phys. Z. **30**, 465 (1929).
[43] D. C. Marinica, A. G. Borisov, and S. V. Shabanov, Phys. Rev. Lett. **100**, 183902 (2008).
[44] I. Rotter and A. F. Sadreev, Phys. Rev. E **71**, 046204 (2005).
[45] A. F. Sadreev, E. N. Bulgakov, and I. Rotter, JETP Lett. **82**, 498 (2005); Phys. Rev. B **73**, 235342 (2006).
[46] E. N. Bulgakov, K. N. Pichugin, A. F. Sadreev, and I. Rotter, JETP Lett. **84**, 430 (2006).
[47] F. M. Dittes, I. Rotter, and T. H. Seligman, Phys. Lett. A **158**, 14 (1991).
[48] *Quantum Chaos and Statistical Nuclear Physics*, edited by T. H. Seligman and H. Nishioka (Springer, Berlin, 1986).
[49] H. Mehri-Dehnavi and A. Mostafazadeh, J. Math. Phys. **49**, 082105 (2008).
[50] R. Pnini and B. Shapiro, Phys. Rev. E **54**, R1032 (1996).
[51] L. Saminadayar, P. Mohanty, R. A. Webb, P. Degiovanni, and C. B. Bäuerle, Physica E (Amsterdam) **40**, 12 (2007); J. J. Lin, T. C. Lee, and S. W. Wang, *ibid.* **40**, 25 (2007); D. S. Golubev and A. D. Zaikin, *ibid.* **40**, 32 (2007).
[52] B. Hackens, S. Faniel, C. Gustin, X. Wallart, S. Bollaert, A. Cappy, and V. Bayot, Phys. Rev. Lett. **94**, 146802 (2005).